

Interference effects on Higgs mass measurement in $e^+e^- \rightarrow H(\gamma\gamma)Z$ at CEPC*

Guang-Zhi Xu(许广智)¹ Gang Li(李刚)² Yi-Jie Li(李一杰)³
Kui-Yong Liu(刘魁勇)³ Yu-Jie Zhang(张玉洁)^{1,4,1)}

¹ Key Laboratory of Micro-nano Measurement-Manipulation and Physics (Ministry of Education) and School of Physics, Beihang University, Beijing 100191, China

² Institute of High Energy Physics, Chinese Academy of Sciences, Beijing 100049, China

³ Department of Physics, Liaoning University, Shenyang 110036, China

⁴ CAS Center for Excellence in Particle Physics, Beijing 100049, China

Abstract: A high luminosity Circular Electron Positron Collider (CEPC) as a Higgs Factory will be helpful for precision measurements of the Higgs mass. The signal-background interference effect is carefully studied for the Higgs diphoton decay mode in associated Z boson production at future e^+e^- colliders at energy 246 GeV. The mass shifts go up from about 20 MeV to 50 MeV for the experimental mass resolution ranging from 0.8 GeV to 2 GeV.

Keywords: keyword, interference effect, Higgs mass, Higgs factories

PACS: 13.66.Fg, 14.80.Bn **DOI:** 10.1088/1674-1137/40/3/033101

1 Introduction

The ATLAS and CMS collaborations at the Large Hadron Collider (LHC) announced the amazing discovery of a new particle with a mass of around 125 GeV in July 2012 [1,2], with properties which are compatible with the Standard Model (SM) Higgs boson [3] but leave room for new physics. One of the next tasks is precision measurements of quantities such as the mass, spin, couplings, and decay patterns, to determine the nature of the Higgs boson. Future e^+e^- colliders such as the International Linear Collider (ILC), a linear particle accelerator, the Triple-Large Electron-Positron Collider (TLEP), and the Circular Electron Positron Collider (CEPC), proposed by the Chinese high energy physics community in 2012, will play an important role in this task.

For future Higgs factories, the $e^+e^- \rightarrow Z^* \rightarrow Z+H(\gamma\gamma)$ process will be an excellent channel for precision measurement. The diphoton decay channel is a rare decay mode but provides a clear signature for the Higgs boson. At the LHC, the $\gamma\gamma$ mode for Higgs production involves a huge background including the dominant reducible jet and the irreducible contributions from the continuum.

The background for measuring the Higgs properties is significantly suppressed at lepton colliders [4]. The Higgsstrahlung process, $e^+e^- \rightarrow ZH$, is the most important process for Higgs production when the center-of-mass energy is less than 500 GeV. With the leading-order calculations, the production cross section of a 125 GeV Higgs reaches its maximum value when the center-of-mass energy is around 246 GeV.

The diphoton decay rate has been calculated up to the complete three-loop level [5] and a four-loop estimation has also been considered [6]. The contributions at the three-loop and four-loop levels can be neglected in comparison with the one-loop decay rate. For the two-loop level, the QCD and electroweak corrections are nearly completely cancelled in the numerical calculations for a Higgs with mass of 125 GeV. The electroweak radiative correction for $e^+e^- \rightarrow ZH$ was calculated [7–9] and the contribution is less than 5% of the tree-level cross section for a Higgs with mass of 125 GeV [9]. For the background from the continuum, the next-to-leading order electroweak corrections have been considered for the $e^+e^- \rightarrow Z\gamma\gamma$ process in the SM by Y. Zhang et al. in a recent work [10]. A correction of 2.32% is observed as the center-of-mass energy is increased to 250 GeV.

Received 25 May 2015, Revised 26 October 2015

* Supported by National Natural Science Foundation of China (11375021, 11447018), New Century Excellent Talents in University (NCET) (NCET-13-0030), Major State Basic Research Development Program of China (2015CB856701), Fundamental Research Funds for Central Universities, and Education Ministry of LiaoNing Province.

1) E-mail: nophy0@gmail.com



Content from this work may be used under the terms of the Creative Commons Attribution 3.0 licence. Any further distribution of this work must maintain attribution to the author(s) and the title of the work, journal citation and DOI. Article funded by SCOAP³ and published under licence by Chinese Physical Society and the Institute of High Energy Physics of the Chinese Academy of Sciences and the Institute of Modern Physics of the Chinese Academy of Sciences and IOP Publishing Ltd

Though the investigation of several typical distributions for the final photons, they also found a dramatic separation between the background and the signal process, which indicated that the background can be significantly suppressed to study the Higgs signal by taking an appropriate kinematic cut.

The interference effects for the Higgs mass in the diphoton decay mode at the hadron colliders have been discussed based on the theoretical aspects. The signal-continuum interference for diphoton final states at the LHC was first studied by L. J. Dixon and M. S. Siu in 2003 [11]. According to S. P. Martin, the mass shift from the interference effect is 150 MeV or more [12], but the effect becomes smaller for final states containing one extra jet [13]. The interference was also evaluated to the next-to-leading order level in recent works [14, 15]. The interference effect of other final states at hadron colliders was also considered in Refs. [16–24].

This work will focus on the interference effect of the Higgs mass through the diphoton decay mode in the Higgs-bremsstrahlung process at the future CEPC e^+e^- collider (for several discussions of the process at CEPC refer to Refs. [25–28] Fan:2014vta, Zhang:2014eqa). Recently, this interference effect with fixed polarisation at the initial state has been considered in Ref. [29], and a mass shift in range of $\mathcal{O}(100 \text{ MeV})$ is found. In this work, the interference effect is revisited with an unpolarized initial state.

2 Calculations and analysis

Figure 1 shows the typical Feynman diagrams for the calculation of interference contributions. The Higgs boson has a very narrow width.

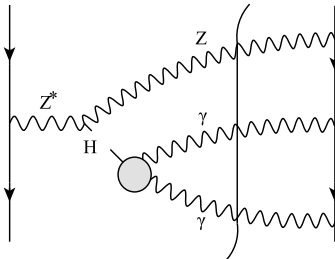


Fig. 1. Typical Feynman diagrams for interference with the continuum.

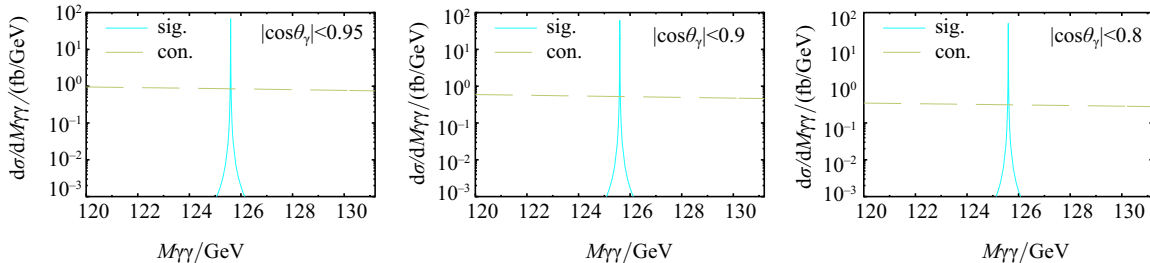


Fig. 2. (color online) Comparison of background and signal process with different cut conditions for the final photons.

Following the method used in Refs. [11–15], with the narrow-width approximation, the pure signal and interference cross sections for the production can be expressed as:

$$\frac{d\sigma^{\text{sig}}}{dM_{\gamma\gamma}} = \frac{|\mathcal{A}_{e^+e^- \rightarrow ZH} \mathcal{A}_{H \rightarrow \gamma\gamma}|^2}{(m_{\gamma\gamma}^2 - m_H^2)^2 + m_H^2 \Gamma_H^2},$$

$$\frac{d\sigma^{\text{int}}}{dM_{\gamma\gamma}} = \frac{-2(m_{\gamma\gamma}^2 - m_H^2)R - 2m_H \Gamma_H I}{(m_{\gamma\gamma}^2 - m_H^2)^2 + m_H^2 \Gamma_H^2}, \quad (1)$$

where R and I represent the real and imaginary parts of the interference amplitude ($\mathcal{A}_{e^+e^- \rightarrow ZH} \mathcal{A}_{H \rightarrow \gamma\gamma} \mathcal{A}_{\text{cont}}^*$), respectively, and $\mathcal{A}_{\text{cont}}^*$ is the continuum amplitude. The real part is odd in the vicinity of the Higgs mass because of the factor $m_{\gamma\gamma}^2 - m_H^2$, and the total contribution to the decay width is negligible. However, as stated in Ref. [12], a sharp peak and a dip exist near the M_H in the diphoton distribution, and the effect slightly moves the peak position. As mentioned in the introduction, the next-to-leading order electroweak corrections to the continuum part contribute less than 5% to the tree-level cross section. Therefore, only the tree-level contribution to the continuum part is considered in our calculation. For the amplitude of the Higgs boson coupled with two photons, we also apply the result at one-loop level [11–14]. For the input parameters, the resonance mass and width of $M_H = 125.6 \text{ GeV}$, $\Gamma_H = 4.2 \text{ MeV}$, the fine structure constant $\alpha = 1/137$, and the running fermion masses $m_t = 168.2 \text{ GeV}$, $m_b = 2.78 \text{ GeV}$, $m_c = 0.72 \text{ GeV}$, $m_\tau = 1.744 \text{ GeV}$ are adopted, respectively. The signal cross section should reach a maximum at around 245–246 GeV. Here we take the center-of-mass energy of 246 GeV in the following calculations.

Figure 2 illustrates the pure signal for diphoton production from Higgs decay, with the continuum cross sections.

Three different cuts on the scattering angle are implemented, which are $|\cos\theta_\gamma^{\text{cut}}| = 0.8$, $|\cos\theta_\gamma^{\text{cut}}| = 0.9$ and $|\cos\theta_\gamma^{\text{cut}}| = 0.95$, respectively. Notably, the experimental cut for the scattering angle may be larger than these values. However, the cross section from ISR, i.e. the continuum contribution, is sensitive to the choice of this kind of cut because its behavior depends on $1/(1 - \cos\theta_\gamma^{\text{cut}})$.

That indicates the background contributions sharply increase compared with the signals when larger angle cuts are chosen, making the interference effect on the mass measurement insensitive to a larger cut. Another cut on the final photon energy is taken to 20 GeV. For the above cut selection, the signal process has a sharp peak in the range 50–70 fb, and the continuum cross section only reaches 0.5–1 fb with the diphoton invariant mass in the range of 120–130 GeV.

The real-part cross sections of the interference as a function of the diphoton invariant mass are shown in Fig. 3(a), whereas the signal with and without the interference effect is shown in Fig. 3(b).

The imaginary part effects are observed to be even

but negligible negative values with their maximum values less than 2% of those of the real part cross sections, and we neglect them in the analysis.

To study the effect of the interference on the Higgs mass measurement, in Ref. [12], convolution integrals with a Gaussian function were added to the cross section to simulate the smearing effect of the Higgs mass due to finite experimental resolution. In Fig. 4, the results are plotted with the Gaussian width as $\sigma_{MR} = 0.8, 1.0, 1.5,$ and 2.0 GeV. Compared with the signals without smearing effects shown in Fig. 3, the peak moves slightly toward the larger mass direction when the interference effects are taken into account. The behavior of the right-side shift is consistent with that shown in [29].

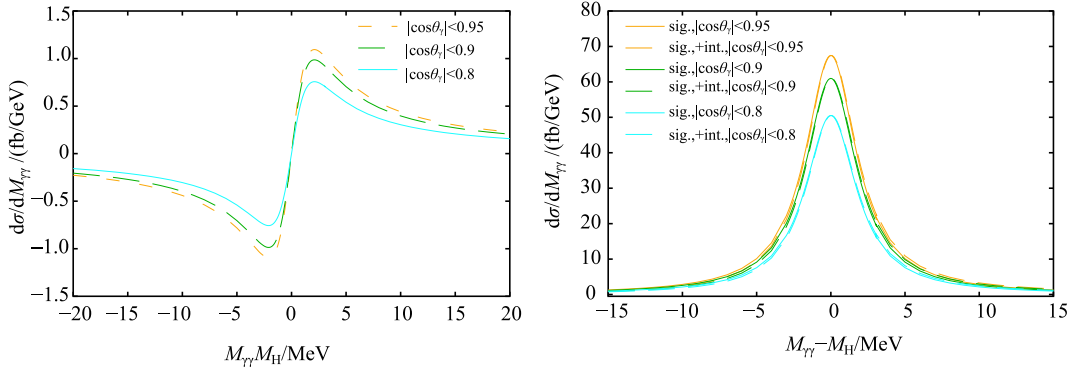


Fig. 3. (color online) (a) the diphoton invariant mass distribution from the real interference and (b) the signal with and without interference from the background. The cut of scattering angle for the photons is chosen as $|\cos\theta_\gamma| < 0.8, |\cos\theta_\gamma| < 0.9$ and $|\cos\theta_\gamma| < 0.95$. The cut of the final photon energy is $E_\gamma > 20$ GeV.

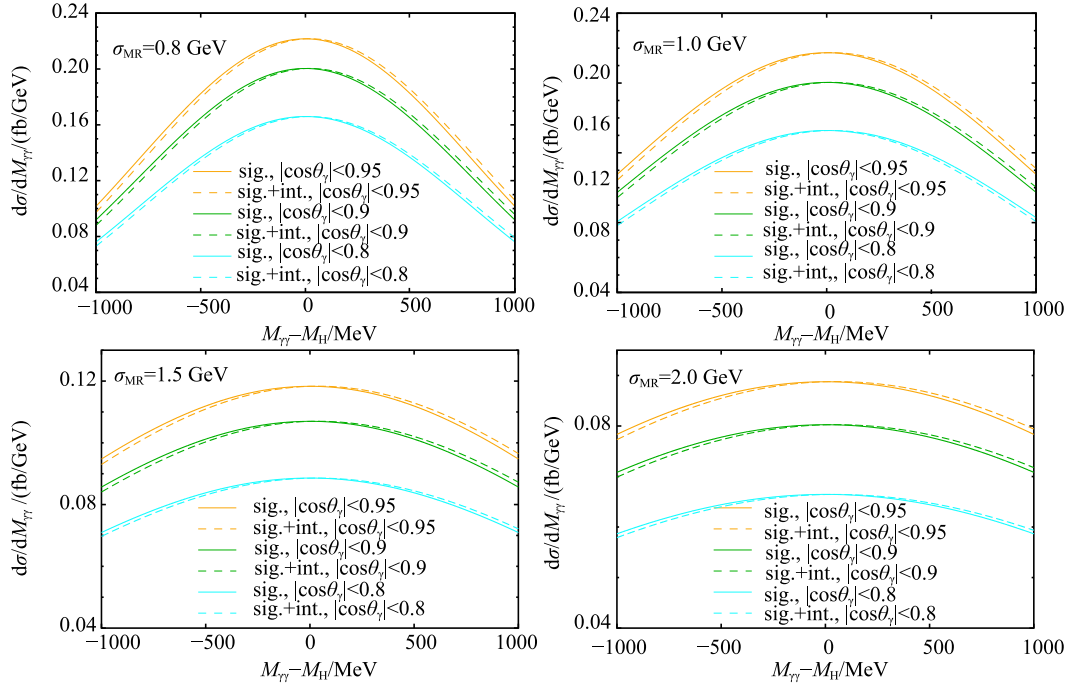


Fig. 4. (color online) Diphoton invariant mass distributions of Higgs signal with different mass resolutions and kinematic cuts. The input parameters, mass resolutions (σ_{MR}) and cut of scattering angle for the photons are noted in the plots. The cut of the final photon energy is $E_\gamma > 20$ GeV.

Similar effects are also observed in previous studies of hadron colliders [11–15] (The left-side or right-side shift effect might occur for different sub-processes).

The strategy stated by S. P. Martin in Ref. [13] is applied to estimate the mass shift, and a least-squares fit to the line shape of mass shifts as a function of the Gaussian width (σ_{MR}) is performed. The results are shown in Fig. 5.

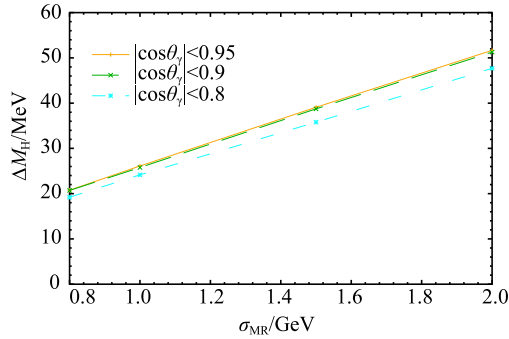


Fig. 5. (color online) The Higgs mass shifts due to the signal-background interference as a function of the Gaussian mass resolution width. Here, a least-squares fit to the line shape of mass shifts is performed according to the strategy proposed by S. P. Martin [13].

Similar to the case of Higgs production in the associated one jet, the mass shifts linearly increase with increasing mass resolution width σ_{MR} [12]. The mass shifts increase from about 20 MeV to 50 MeV, corresponding to the range of the mass resolution width from 0.8 GeV to 2.0 GeV. From the figure, the two lines corresponding to the final photon scattering angle cut $|\cos\theta_{\gamma}^{\text{cut}}| = 0.9$ and

$|\cos\theta_{\gamma}^{\text{cut}}| = 0.95$, respectively, are very close to each other in comparison with the line for $|\cos\theta_{\gamma}^{\text{cut}}| = 0.8$. This result implies that the shifts from the interference effect are not sensitive to a larger angle cut, as mentioned in the above analysis.

Different from the calculations at a linear collider with polarized beams in a recent paper [29], we focus on the CEPC collider with unpolarized beam in the energy range from 240 GeV to 250 GeV. However, we can still compare our results with the results at $\sqrt{s} = 250$ GeV in [29]. Similar right-side shifts in the Higgs mass as stated in Ref. [29] were also observed in our paper. To determine the magnitude of the shifts, the authors of Ref. [29] applied the method proposed by Ref. [12] and an experimental interval for the spectrum measurement was introduced in this method. In contrast, we followed the strategy in Ref. [13] to perform a least-squares fit.

3 Summary

In this work, following the previous works regarding hadron colliders [11–15], the signal-background interference effect of the Higgs mass through diphoton decay mode in associated Z boson production at future e^+e^- colliders at energy 240 ~ 250 GeV was considered. Different cut conditions for the final photon scattering angle and different smearing width to simulate the experiments were also considered. Considering the smearing Gaussian width σ_{MR} (which simulated the experimental mass resolution) ranging from 0.8 GeV to 2 GeV, the corresponding mass shifts increased from about 20 MeV to 50 MeV. These results will be beneficial in precision measurements of the Higgs mass.

References

- 1 S. Chatrchyan et al (CMS Collaboration), Phys. Lett. B, **716**: 30-61 (2012)
- 2 G. Aad et al (ATLAS Collaboration), Phys. Lett. B, **716**: 1-29 (2012)
- 3 S. Dawson, A. Gritsan, H. Logan et al, arXiv: 1310.8361
- 4 X. Mo, G. Li, M. Q. Ruan et al, arXiv:1505.01008
- 5 P. Maierhofer and P. Marquard, Phys. Lett. B, **721**: 131 (2013)
- 6 C. Sturm, Eur. Phys. J. C, **74**(8): 2978 (2014)
- 7 A. Denner, B. A. Kniehl, and J. Kublbeck, Nucl. Phys. Proc. Suppl. A, **29**:263-269 (1992)
- 8 A. Denner, J. Kublbeck, R. Mertig, and M. Bohm, Z. Phys. C, **56**:261-272 (1992)
- 9 C. Englert and M. McCullough, JHEP, **1307**:168 (2013)
- 10 Y. Zhang, L. Guo, W. G. Ma et al, Eur. Phys. J. C, **74**:2739 (2014)
- 11 L. J. Dixon and M. S. Siu, Phys. Rev. Lett., **90** :252001 (2003)
- 12 S. P. Martin, Phys. Rev. D, **86**: 073016 (2012)
- 13 S. P. Martin, Phys. Rev. D, **88**: 013004 (2013)
- 14 L. J. Dixon and Y. Li, Phys. Rev. Lett., **111**: 111802, (2013)
- 15 D. de Florian, N. Fidanza, R. J. Hernández-Pinto et al, Eur. Phys. J. C, **73**(4): 2387 (2013)
- 16 J. M. Campbell, R. K. Ellis and C. Williams, JHEP, **1404**: 060 (2014)
- 17 J. M. Campbell, R. K. Ellis and C. Williams, Phys. Rev., D, **89**: 053011 (2014)
- 18 J. M. Campbell, R. K. Ellis and C. Williams, JHEP, **1110**: 005 (2011)
- 19 J. M. Campbell, R. K. Ellis, E. Furlan et al, Phys. Rev. D, **90**: 093008 (2014)
- 20 P. Niezurawski, A. F. Zarnecki, and M. Krawczyk, JHEP, **0211**: 034 (2002)
- 21 D.A. Morris, T.N. Truong, and D. Zappala, Phys. Lett. B, **323**: 421-426 (1994)
- 22 D. Dicus, A. Stange, and S. Willenbrock, Phys. Lett. B **333**: 126-131 (1994)
- 23 N. Kauer and C. O'Brien, arXiv:1502.04113
- 24 S. Jung, J. Song, and Y. W. Yoon, arXiv:1505.00291
- 25 Q. L. Xiu, H. B. Zhu and X. C. Lou, arXiv:1505.01270
- 26 M. Q. Ruan, arXiv:1411.5606
- 27 J. J. Fan, M. Reece and L. T. Wang, arXiv:1411.1054
- 28 Y. Zhang, K. Ohmi, D. Zhou, and D. Shatilov, Beam-Beam Simulation Study for CEPC. p. THPRI003 (2014)
- 29 S. Liebler, arXiv:1503.07830